Reduction of $A\beta_{25-35}$-Induced Cognitive Impairments in C57BL/6 Mice Through Focused Ultrasound Thermal-Cycling Stimulation

Guan-Bo Lin[1,2], Hsu-Hsiang Liu[2,3], Yu-Yi Kuo[1,2], You-Ming Chen[2,3], Fang-Tzu Hsu[1,2], Yu-Wei Wang[2,3], Yi Kung[2,3], Chien Ching[2,3] and Chih-Yu Chao[1,2,3]*

[1] Department of Physics, Laboratory for Medical Physics & Biomedical Engineering, National Taiwan University, Taipei 106319, Taiwan; gblin@phys.ntu.edu.tw (G.B.L.); hhliu@phys.ntu.edu.tw (H.H.L.); yykuo@phys.ntu.edu.tw (Y.Y.K.); ymchen@phys.ntu.edu.tw (Y.M.C.); tsyr8924503@phys.ntu.edu.tw (F.T.H.); f10245021@phys.ntu.edu.tw (Y.W.W.); a13956@phys.ntu.edu.tw (Y.K.); albertj8808@phys.ntu.edu.tw (C.C.); cychao@phys.ntu.edu.tw (C.Y.C.)

[2] Molecular Imaging Center, National Taiwan University College of Medicine, Taipei 100233, Taiwan

[3] Graduate Institute of Applied Physics, Biophysics Division, National Taiwan University, Taipei 106319, Taiwan

***** Correspondence: Chih-Yu Chao

Department of Physics, Lab for Medical Physics and Biomedical Engineering, National Taiwan University, No 1, Sec 4, Roosevelt Rd., Taipei 106319, Taiwan, Republic of China

Tel +886-2-3366-9612

Fax +886-2-3366-5088

E-mail: cychao@phys.ntu.edu.tw (CYC)

Abstract

Hyperthermia (HT) is recognized across various medical disciplines for its capacity to modulate specific protein expressions. In efforts to improve Alzheimer's disease (AD), HT has the potential to regulate heat shock proteins (HSPs) and antioxidant enzymes, which helps decrease the aberrant accumulation of β-amyloid (Aβ) protein and oxidative stress. Nonetheless, the precise delivery of mild hyperthermia to the brain remains a significant challenge. To apply mild hyperthermia targeted to the brain and evaluate its impact on cognitive improvement, this study used focused ultrasound (FUS) to administer localized mild hyperthermia to the brains of AD mouse induced by intracerebroventricular (i.c.v.) injection of $A\beta_{25\text{-}35}$. For considerations of safety and therapeutic efficacy, a thermal-cycling hyperthermia (TC-HT) protocol was adapted into a focused ultrasound thermal-cycling stimulation (FUS-TCS), which was compared with the continuous focused ultrasound hyperthermia stimulation (FUS-HTS). The findings revealed that the FUS-TCS treatment group exhibited a significant improvement in cognitive performance, as evidenced by enhanced outcomes in the Y-maze and novel object recognition (NOR) tests. Furthermore, this group demonstrated increased expression of Aβ-degrading enzymes and antioxidant proteins, including heat shock protein 70 (HSP70), neprilysin (NEP), insulin degrading enzyme (IDE), sirtuin 1 (SIRT1), and superoxide dismutase 2 (SOD2). These results suggest that localized mild hyperthermia targeting the brain using FUS-TCS treatment represents a promising strategy for ameliorating cognitive deficits associated with AD.

Introduction

Hyperthermia (HT) represents a non-pharmacological approach to modulating biological responses by inducing alterations in cellular signaling pathways through temperature variations [1-3]. Various modalities of hyperthermia have been extensively applied in the treatment of diverse conditions, including muscle pain, arthritis, inflammatory disorders, and cancer [3-5]. In the realm of neurodegenerative diseases, hyperthermia has emerged as a potential therapeutic strategy for

health improvement [6,7]. Alzheimer's disease (AD), the most prevalent neurodegenerative disorder, is characterized by progressive cognitive decline and is experiencing a rising incidence globally. The aberrant accumulation of β-amyloid (Aβ) peptides in the brain is widely recognized as a major pathogenic factor in AD, contributing to oxidative stress, neuronal injury, and subsequent cognitive deficits [8-10]. Consequently, interventions targeting the mitigation of oxidative stress and the reduction of pathological Aβ depositions have garnered significant research interest [10-14].

Several protective proteins, which can be upregulated in response to hyperthermia, may underlie its capacity to mitigate Aβ accumulation and oxidative stress. Among these protective proteins, heat shock proteins (HSPs), particularly heat shock protein 70 (HSP70), are well-characterized molecular chaperones that are inducible by thermal stimulation. HSP70 contributes to the maintenance of protein homeostasis by preventing Aβ misfolding and aggregation, thereby facilitating its clearance [15,16]. Additionally, certain proteins known as Aβ-degrading enzymes, including neprilysin (NEP) and insulin-degrading enzyme (IDE), are implicated in the degradation and removal of Aβ, with their upregulation potentially contributing to the amelioration of AD pathology [12,17]. In addition to targeting Aβ, the regulation of oxidative stress represents another critical focus in AD pathogenesis. Proteins such as sirtuin 1 (SIRT1) and superoxide dismutase 2 (SOD2) play pivotal roles in modulating oxidative stress levels, thereby influencing the progression of AD [18,19]. Notably, several of the aforementioned protective proteins, including HSP70 and IDE, can be upregulated by hyperthermia, suggesting mechanistic pathways through which hyperthermia may confer neuroprotection and cognitive benefits [20-22]. These findings offer valuable insights into potential strategies for the prevention or mitigation of AD. Moreover, a Finnish study suggests that frequent use of Finnish saunas, particularly at moderate to high frequencies, may be associated with a reduced risk of developing AD [23]. Collectively, these observations position hyperthermia as a promising intervention capable of modulating key protein pathways implicated in AD, thereby offering potential therapeutic benefits.

Although these findings are encouraging, the majority of previous investigations have concentrated on in vitro experiments or whole-body hyperthermia techniques. The advancement of methodologies for the precise and safe application of hyperthermia to the brain remains underdeveloped, posing a significant obstacle to clinical translational. Focused ultrasound (FUS) offers a potential solution to this problem by directing ultrasound waves to a confined focal region, thereby minimizing effects on adjacent tissues. Clinically, high-intensity focused ultrasound (HIFU) enables noninvasive ablation of solid tumors by elevating focal temperatures above 55 °C, sometimes reaching 65 °C or even 80°C, resulting in coagulative necrosis [24-26]. Moreover, HIFU is employed in medical aesthetics to target the deep dermis and superficial musculoaponeurotic system, where focal heating to approximately 60–70 ℃ induces collagen denaturation and contraction, facilitating skin tightening and rejuvenation [27,28]. In the context of brain applications, prior research has primarily utilized low-energy FUS for neural modulation or employed microbubbles to transiently disrupt the blood-brain barrier (BBB) to enhance drug delivery, rather than for thermal effects [29,30]. Different from both high-temperature HIFU and non-thermal low-energy FUS, we propose the use of FUS to induce mild hyperthermia in the brain through moderately elevated temperatures. Compared to whole-body hyperthermia, localized brain warming, as demonstrated in studies targeting brain tumors to improve drug delivery, allows for more precise stimulation of specific brain regions while limiting thermal exposure to surrounding tissues [31,32]. Nonetheless, prolonged exposure to elevated temperatures can exert thermotoxic effects on neural cells [33,34], and investigations into the neuroprotective potential of mild brain hyperthermia for neuroprotection remain scarce. Therefore, establishing a tolerable, effective, and safe approach for targeted brain hyperthermia is of critical importance for advancing AD research.

In our previous investigations, we introduced a novel therapeutic approach termed thermal cycling hyperthermia (TC-HT), which demonstrated neuroprotective effects in vitro and was shown to be more efficacious than conventional hyperthermia (HT) [35,36]. Furthermore, in an animal study, we administered heat energy to the heads of mice using polyimide thermofoil and observed

that intermittent heat treatment via TC-HT significantly improved cognitive function compared to continuous HT [37]. Building upon this prior external head-heating technique, the present study employed focused ultrasound thermal-cycling stimulation (FUS-TCS) to deliver thermal energy directly to specific brain regions. The safety profile of FUS-TCS was assessed in comparison to continuous focused ultrasound hyperthermia stimulation (FUS-HTS). Cognitive performance in C57BL/6 mice exhibiting $A\beta_{25–35}$–induced impairments was evaluated following FUS-TCS treatment using the Y-maze and novel object recognition (NOR) tests. Concurrently, we examined the expression of heat- and stress-responsive proteins implicated in Aβ clearance, including HSP70, IDE, and NEP, as well as antioxidant-related proteins such as SIRT1 and SOD2, which play critical roles in oxidative stress regulation. The results indicate that FUS-TCS may mitigate Aβ-induced cognitive deficits and modulate key proteins involved in AD pathology, thereby providing a promising framework for further preclinical evaluation and therapeutic development.

Results

Temperature assessment on the phantom during FUS-TCS application

To demonstrate the thermal distribution induced by FUS, a thermochromic phantom was utilized for visualizing temperature-dependent responses. The phantom consisted of a transparent portion and a white region containing thermochromic powder, which enabled visual observation of local heating through a color change near 40.0 ℃. As shown in Figure 1A, the thermochromic region appeared approximately 8 mm distal to the transducer aperture, with a diameter of about 2–3 mm, when the FUS transducer operated at 1.2 MHz. In contrast, at 1.8 MHz, the color change occurred approximately 15 mm away from the aperture, with the thermochromic region measuring about 1 mm in diameter, as depicted in Figure 1B. These results demonstrate that FUS is capable of delivering thermal energy to a specific target region, and that different operating frequencies result in distinct focal zones of energy deposition. To ensure that the targeted brain region of mice received mild hyperthermia in subsequent experiments, we selected an operating frequency of

1.2 MHz to better cover the mouse brain. Prior to applying FUS-TCS to the mice, we first measured the temperature profile in the phantom. As shown in Figure 1C, during the 3-minute high-temperature phase of FUS-TCS, the temperature of the heating region was maintained at 40.0 ± 0.5 °C, followed by a rapid decrease to approximately 34.0 °C during the 1-minute resting phase. Collectively, the phantom results supported the selection of FUS-TCS parameters that ensure reliable and steady thermal energy delivery in the subsequent animal experiments.

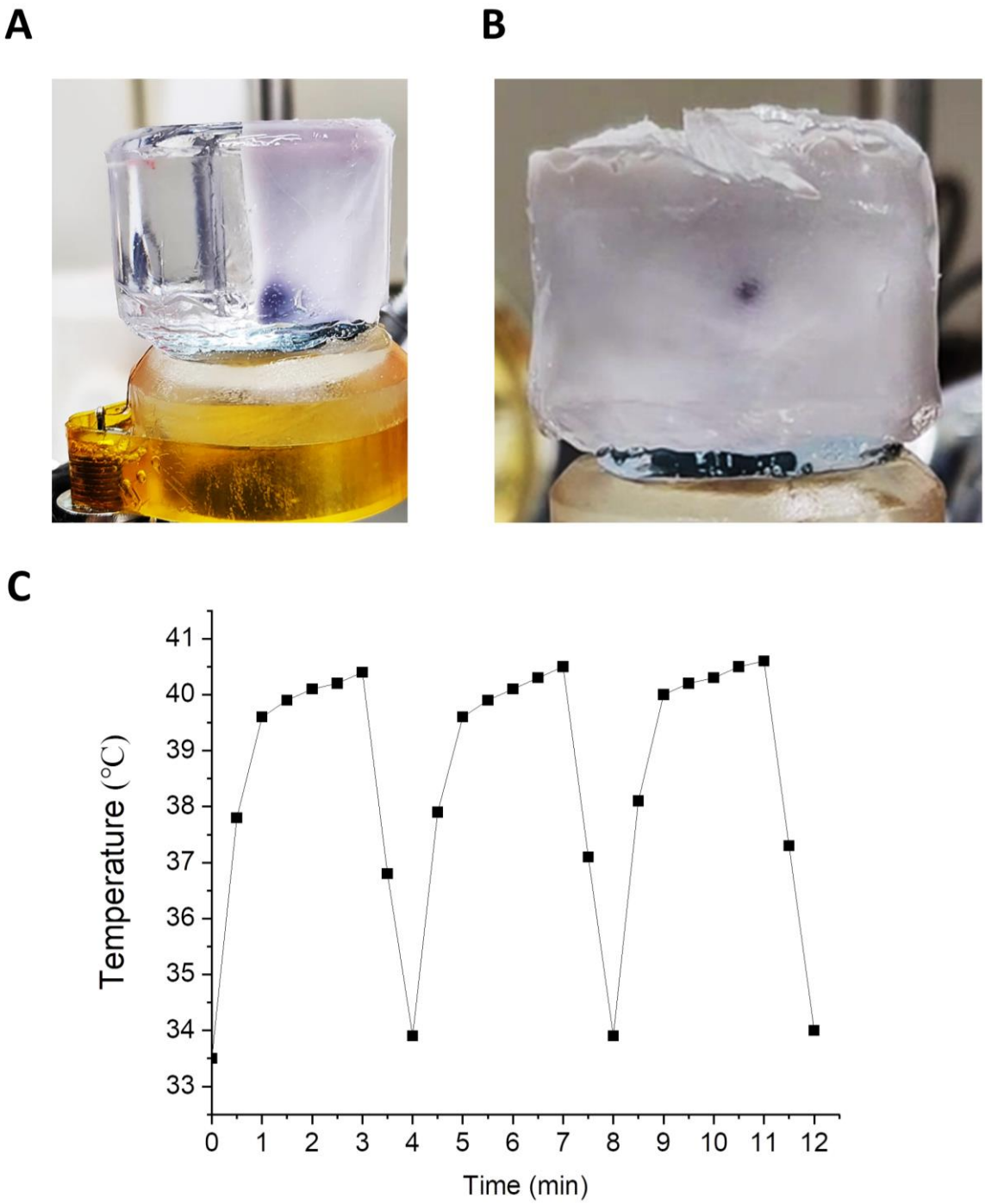

Figure 1. Representative thermochromic responses and temperature measurements in the phantom under FUS exposure. Colorimetric changes were observed in the thermochromic phantom following FUS application at (A) 1.2 MHz and (B) 1.8 MHz. (C) Temperature profile recorded in the phantom during FUS-TCS application at 1.2 MHz. The white region of the phantom was fabricated using an acrylamide-based hydrogel formulation containing thermochromic powder that undergoes a visible color transition at 40.0 ℃. Temperature was measured using a K-type thermocouple embedded at the geometric center of the thermal focal zone.

- **In vivo mice brain temperature monitoring and experimental schedule**

Prior to conducting subsequent experiments, we evaluated the temperature profiles in the mouse brain during FUS exposure to confirm the delivery of controlled mild hyperthermia. The temperature measurements were performed under anesthesia using a K-type thermocouple inserted into the mouse brain. As shown in Figure 2A, for the FUS-TCS application, a 10-cycle repeated procedure was implemented. Each cycle consisted of a high-temperature phase lasting 3 minutes, during which the temperature was maintained at 39 ± 1 °C with a peak temperature of approximately 40 °C, followed by a 1-minute passive cooling phase in which the temperature rapidly decreased. For HT application, the temperature maintained at 40 ℃ for 30 min. These results suggested that mild hyperthermia could be well-controlled achieved through FUS application. Following the confirmation of thermal feasibility, subsequent animal experiments were conducted according to a predefined schedule. As illustrated in Figure 2B, Aβ solution was administered via i.c.v. injection into the brains of mice in the Aβ, FUS-TCS, and FUS-HTS groups on day 0. Thermal applications were applied to the FUS-TCS and FUS-HTS groups on days 4, 8, and 12. Behavioral evaluations were then conducted, including spontaneous alternation in the Y-maze to assess locomotor activity and short-term spatial working memory on day 13. In addition, NOR tests were performed on days 14 and 15 to evaluate short-term (1 h) and long-term (24 h)

memory, respectively. These assessments leverage mice's natural tendency to explore novel environments or unfamiliar objects [38-41].

Figure 2. Temperature assessment in the mouse brain under FUS stimulation and experimental timeline. (A) Representative temperature profiles recorded from the mouse brain during FUS-TCS and continuous FUS-HTS application. Measurements were performed under anesthesia using a K-type thermocouple inserted into a small cranial opening. The temperature traces shown reflect the stabilized temperatures achieved during FUS application, with FUS-HTS maintained at approximately 40 °C and FUS-TCS fluctuating between 35-40 °C. Notably, brain temperature reached the target range within the first TC-HT cycle and was maintained in subsequent cycles. (B) Schematic representation of the experimental schedule. Mice were euthanized for brain tissue collection 24 hours after the NOR test on day 15.

Effects of thermal treatments on behavioral performance in mice

Prior to conducting cognitive assessments in AD mice, we first evaluated the safety of two hyperthermic stimulation approaches, FUS-TCS and FUS-HTS. As illustrated in Figure 3A, no significant differences were observed in the number of arm entries in the Y-maze test between the two thermal stimulation groups, indicating that these treatments did not affect the locomotor activity of the mice. However, the FUS-HTS group exhibited a lower spontaneous alternation index (51.0%) compared to the control group (60.4%), whereas no significant difference was observed between the FUS-TCS and control groups (Figure 3B). Additionally, as shown in Figures 3C and 3D, both short-term (1 h) and long-term (24 h) discrimination indexes in the NOR test were reduced in the FUS-HTS group compared to the control group, decreasing from 63.1% to 42.1% at 1 h and from 61.7% to 42.6% at 24 h tests, respectively. Conversely, the FUS-TCS group maintained discrimination index comparable to those of the control group at both time points, indicating preserved cognitive performance. These results suggest that continuous thermal stimulation

FUS-HTS may diminish cognitive performance, whereas intermittent mild hyperthermia FUS-TCS appears to preserve cognitive function. Therefore, FUS-TCS was selected for subsequent investigations in AD mice.

Figure 3. Effects of FUS-TCS and FUS-HTS treatments on mice behavioral performances. Behavioral outcomes under different types of thermal applications were evaluated by (A) total number of arm entries and (B) spontaneous alternation index in the Y-maze test, as well as (C) discrimination index at 1 h and (D) 24 h intertrial intervals in the NOR test. Data are presented as mean ± SEM. Statistical significance was assessed by one-way ANOVA with Tukey's post-hoc test. Significance between groups is indicated as *P < 0.05, **P < 0.01, while non-significant differences are labeled ns.

FUS-TCS treatment attenuates Aβ-induced cognitive deficits in mice

To evaluate the potential of mild hyperthermia achieved through FUS-TCS in modulating Aβ-induced cognitive changes, behavioral assessments were conducted using the Y-maze and NOR tests. As shown in Figure 4A, there was no significant difference in the total number of arm entries among the control, Aβ, and Aβ+FUS-TCS groups, indicating comparable locomotor activity. In contrast, Figure 4B illustrates that Aβ-injected mice exhibited a spontaneous alternation index decreased from 63.0% in controls to 50.4%, suggesting impaired working memory. Notably, FUS-TCS improved the alternation performance that was reduced by Aβ, with levels approaching those of the control group. In addition, as shown in Figure 4C, Aβ-injected mice exhibited a decreased discrimination index at the 1 h intertrial interval in NOR test, decreased from 60.8% to 28.2%. In contrast, discrimination performance in the Aβ+FUS-TCS group improved to 55.8%, showing no statistical difference from control. Similarly, at the 24 h intertrial interval NOR test (Figure 4D), the Aβ group exhibited a markedly reduced discrimination index (12.4%), whereas application of Aβ+FUS-TCS led to a substantial recovery to 56.2%, which was not significantly

different from that of the control group. Collectively, these results suggest that FUS-TCS may attenuate Aβ-associated deficits in recognition memory. Building on these behavioral improvements, we next examined whether FUS-TCS modulates molecular pathways involved in Aβ clearance and antioxidant defense.

Figure 4. FUS-TCS mitigates Aβ-induced cognitive deficits in mice.

Behavioral assessments were performed to evaluate locomotor activity and cognitive function among control, Aβ, and Aβ + FUS-TCS groups. The Y-maze test measured (A) total arm entries and (B) spontaneous alternation index, while the NOR test assessed recognition memory through (C) 1-hour and (D) 24-hour discrimination indices. Results are presented as mean ± SEM. Significance was analyzed using one-way ANOVA with Tukey's post-hoc test. $^{**}P < 0.01$, $^{***}P < 0.001$, while non-significant differences are labeled ns.

Modulation of Aβ accumulation and clearance-related proteins by FUS-TCS

Given that Aβ accumulation is a hallmark of AD and that FUS-TCS improved behavioral performance in Aβ-injected mice, we sought to investigate whether this treatment modulates Aβ levels and the expression of clearance-associated proteins in the hippocampus. As shown in Figure 5A, Aβ-injected mice exhibited a significant increase in hippocampal Aβ expression, reaching 1.74-fold relative to controls. Notably, FUS-TCS treatment significantly reduced Aβ levels compared to the Aβ-only group, decreasing to control levels. Following the evaluation of Aβ levels, we assessed the expression of Aβ clearance-related proteins. As shown in Figure 5B, hippocampal HSP70 expression in Aβ-injected mice was slightly elevated but not significantly different from the control group, whereas FUS-TCS treatment significantly increased HSP70 levels compared to both the control and Aβ groups, reaching 1.57-fold relative to control. Furthermore, IDE, a well-known Aβ-degrading enzyme was investigated. It has been suggested that reduced IDE expression may be linked to Aβ accumulation in AD, and restoring IDE levels could potentially attenuate this effect

[42,43]. In this study, as illustrated in Figure 5C, the Aβ group exhibited a significant downregulation of IDE expression, decreasing to 0.63-fold relative to the control group. In contrast, a marked recovery of IDE expression was observed in the FUS-TCS treatment group, reaching 0.99-fold of control levels without statistical difference. In addition to IDE, NEP is also recognized as a key Aβ-degrading enzyme involved in Aβ clearance [44,45]. Downregulation of NEP has been implicated in Aβ accumulation, whereas increasing NEP expression may attenuate Aβ levels in models of AD [46-48]. In this study, our results demonstrated that NEP expression was markedly reduced following Aβ administration, reaching 0.58-fold of control levels, and this decrease was ameliorated by FUS-TCS treatment, as depicted in Figure 5. Taken together, these findings suggest that FUS-TCS may modulate key molecular pathways involved in Aβ clearance, potentially contributing to the cognitive improvements observed in treated mice.

Figure 5. Effect of FUS-TCS applications on the expression levels of Aβ, HSP70, IDE, and NEP in the mice hippocampus. Representative western blots and quantification of (A) Aβ, (B) HSP70, (C) IDE, and (D) NEP expression in the mice hippocampus to assess the anti-Aβ effect. β-actin was used as an internal control. Relative expression levels were normalized to the control group and expressed as fold changes. Data are presented as mean ± standard error of the mean. Statistical significance was determined using one-way ANOVA followed by Tukey's post-hoc test. Significance between indicated groups is denoted as **P < 0.01, ***P < 0.001, while non-significant differences are labeled as ns.

Expression of antioxidant-related proteins SIRT1 and SOD2 following FUS-TCS

Oxidative stress resulting from elevated levels of reactive oxygen species (ROS) contributes significantly to neuronal damage and the progression of AD, highlighting the importance of oxidative stress regulation in therapeutic strategies [49-51]. SIRT1, a NAD^+-dependent deacetylase, plays a key role in regulating cellular defense mechanisms by modulating multiple downstream

pathways involved in antioxidant and anti-inflammatory responses [52,53]. Previous studies have reported that SIRT1 expression is downregulated in AD patients and negatively correlated with Aβ accumulation [54,55]. Evidence indicates that SIRT1 upregulation is associated with reduced Aβ accumulation and may ameliorate AD pathology in in vivo models [56-58]. In this study, as shown in Figure 6A, SIRT1 expression in the Aβ group was reduced to 0.73-fold relative to the control. This reduction was ameliorated in the FUS-TCS treatment group, in which SIRT1 levels showed no significant difference compared to the control group. Furthermore, antioxidant protein SOD2 is a well-known downstream target of SIRT1-regulated antioxidant pathways, and studies have shown that increased SIRT1 expression can elevate SOD2 levels [59-61]. In addition, research has suggested that SOD2 is capable of reducing hippocampal superoxide levels and amyloid plaque burden in AD mice [62]. As shown in Figure 6B, SOD2 expression was significantly reduced to 0.60-fold of the control group, whereas FUS-TCS treatment restored its expression to control levels without significant difference. These findings demonstrated that FUS-TCS restored the expression of key antioxidant-related proteins SIRT1 and SOD2 in the hippocampus, implying a possible role in mitigating oxidative stress.

Figure 6. Effects of FUS-TCS treatment on the expression of antioxidant-related proteins SIRT1 and SOD2 in the mouse hippocampus. Representative western blots and quantification of (A) SIRT1 and (B) SOD2 expression in the mice hippocampus to assess antioxidant effects. β-actin was used as an internal control. Relative expression levels were normalized to the control group and expressed as fold changes. Data are presented as mean ± standard error of the mean. Statistical significance was determined using one-way ANOVA followed by Tukey's post-hoc test. Significance between indicated groups is denoted as **P < 0.01, ***P < 0.001, while non-significant differences are labeled as ns.

Discussion

AD is a major cause of dementia, and with the aging population, the threat it poses to humanity is becoming increasingly severe. Scientists are devoted to seeking effective treatments, with the most prominent strategy being to eliminate Aβ [63,64]. However, due to the presence of the BBB, application of drugs becomes immensely difficult, while the resulting side effects also present a considerable challenge [65,66]. Therefore, finding promising alternative therapies is critical.

Hyperthermia emerges as an optimistic non-drug candidate, as appropriate thermal stimulation promotes neuroprotection [67,68]. Nevertheless, how to apply thermal energy into the brain specifically and activate related neuroprotective pathways is an issue worthy of research. In contrast to whole-body hyperthermia, in our previous study, we applied thermal stimulation directly to the heads of mice using polyimide thermofoil, which improved recognition dysfunction [37]. In this study, we take a step further, applying thermal stimulation into the brain of mice directly via FUS, aiming to regulate protein expressions and ameliorate cognitive impairment. In addition, to avoid the damage of excessive heat stimulation, our team is dedicated to developing an improved method of thermal stimulation, which we refer to as TC-HT. This approach preserves the benefits of thermal stimulation through intermittent heat cycling while reducing the accumulation of excessive stress. Our previous studies have verified the safety of TC-HT and its effect is better than traditional HT, both in vitro and in vivo [35-37]. This study also implemented the concept of TC-HT, which is termed as FUS-TCS. The application of FUS-TCS did not adversely affect the mice's health or exploratory behavior in the Y-maze and NOR tests. Notably, it even enhanced the success rate of spontaneous alternation in the Y-maze. In contrast, mice subjected to FUS-HTS exhibited a relatively lower success rate (Figure 2). These results support the behavioral benefits of FUS-TCS and indicate that it is a safe stimulation modality in vivo.

Considering that cognitive impairment is a hallmark of AD, we subsequently evaluated the effects of FUS-TCS on the performance of behavioral tests in Aβ-induced cognitive impairment mice. The results revealed that FUS-TCS applications significantly enhanced the spontaneous index of mice in the Y-maze test compared to the Aβ group (Figure 3). Additionally, in the NOR test,

cognitive impairment induced by Aβ was effectively ameliorated by FUS-TCS applications encompassing tests for both short-term and long-term memory (Figure 4). These in vivo test outcomes indicated the potential of FUS-TCS in improving memory deficiency and cognitive dysfunction induced by Aβ.

The removal of Aβ has always been a major objective in AD treatment research. This study found that FUS-TCS applications can ameliorate Aβ-induced cognitive impairment in mice (Figure 3 and 4), as well as reduced the expression level of Aβ in the hippocampus (Figure 5A). The underlying mechanism may involve the regulation of protective proteins by thermal stimulation. Among these, HSP70, a major heat shock protein, plays a central role in proteostasis by assisting in the refolding and degradation of misfolded proteins, and has been reported to reduce Aβ aggregation and promote its elimination [6,15,69,70]. The study found that the FUS-TCS group exhibited a significant upregulation in the expression level of HSP70 in the hippocampus compared to the Aβ group (Figure 5B). In addition to HSP70, Aβ-degrading enzymes such as IDE and NEP also play a crucial role in the clearance of Aβ [12,17]. The role of IDE in AD has garnered considerable attention, with both in vitro and in vivo studies demonstrating its capacity to reduce Aβ accumulation [46,71-73]. Notably, IDE has been suggested to exhibit characteristics similar to HSPs, which increases its expression levels after heat stimulation [22], and our previous study also suggested that applying thermal stimulation to mouse heads via polyimide thermofoil could increase the expression of IDE in the mouse hippocampus [37]. Moreover, in this study we also found that application of FUS-TCS significantly recovered the Aβ-induced decline in IDE (Figure 5C), reinforcing the potential therapeutic role of FUS-TCS in AD. Additionally, NEP is another Aβ-degrading enzyme expressed in the brain that has also gathered significant attention. The decline in NEP expression during AD progression is associated with Aβ accumulation, whereas NEP overexpression has been shown to promote Aβ degradation [46-48,71,72]. In present study, we applied thermal stimulation using FUS-TCS and found that it could recover NEP expression

impaired by Aβ (Figure 5D). These findings suggest that FUS-TCS may promote the expression of proteins involved in Aβ clearance, thereby increasing its potential to ameliorate AD pathology.

Regulation of oxidative stress is another important aspect of AD research. SIRT1, a NAD^+-dependent deacetylase, has emerged as a key regulator of oxidative stress, mitigating ROS accumulation and contributing to neuroprotection [74,75]. Studies have reported that SIRT1 expression is reduced in AD patients [55, 76,77]. Conversely, increased expression of SIRT1 has been shown to alleviate oxidative stress and contribute to the mitigation of Aβ accumulation [58,78]. In this study, our results showed that FUS-TCS application upregulated SIRT1 levels (Figures 6A). Additionally, SIRT1 has been suggested to upregulate SOD2, a key mitochondrial scavenger for superoxide, thereby promoting antioxidant defense, with elevations of both proteins also observed in cells exhibiting increased stress resistance [61,79]. In our study, FUS-TCS treatment increased the expression of SOD2 (Figure 6B), supporting the potential of this approach to alleviate oxidative stress in the AD mouse model. These results highlight the potential of FUS-TCS to enhance antioxidant proteins and its potential for improving AD.

Thermal stimulation exerts physical effects on biological systems by altering temperature, which in turn modulates cellular functions and key signaling pathways. It has demonstrated benefits in pain control and cancer therapy, and growing evidence suggests its potential neuroprotective role [68,80-82]. A critical aspect of applying thermal stimulation to the brain is the ability to deliver localized heating while maintaining precise control over the thermal dose to avoid potential adverse effects. In our previous study, heat energy was delivered to the heads of mice using a polyimide thermofoil, and the results indicated that thermal cycling hyperthermia (TC-HT) enhanced cognitive performance [37]. However, this method indirectly heats the brain through conduction rather than direct targeting [37]. Given the small size and thin skull of mice, this approach effectively influences brain proteins, although there remains room for improvement. To address this, the present study employs FUS as a thermal stimulation modality, utilizing the focal energy of ultrasound to directly and precisely regulate temperature within the brain. Additionally, to prevent

excessive accumulation of heat energy, we incorporated the TC-HT method, which introduces intermittent cooling periods during thermal stimulation. This cyclic method reduces the risk of thermal damage that may be caused by traditional HT through rest and cooling intervals during thermal stimulation. This approach preserves the beneficial effects of thermal stimulation while improving safety (Figure 2). The study demonstrated that application of FUS-TCS could improve the spatial cognition and learning deficits in vivo (Figure 3 and 4). For the molecular mechanism, we found that the application of FUS-TCS significantly upregulated several proteins involved in Aβ clearance, including the molecular chaperone HSP70, as well as Aβ-degrading enzymes IDE and NEP (Figures 5B–5D), which may contribute to the observed decline in Aβ levels (Figure 5A). Furthermore, FUS-TCS could increase the expression of SIRT1 and SOD2 (Figure 6A and 6B), suggesting a potential involvement in oxidative stress regulation, which might also contribute to the improvement of cognitive deficits (Figure 3 and 4). In summary, the present study provides preliminary evidence that FUS-TCS may serve as a feasible approach for delivering localized thermal stimulation to the brain. Additionally, it may offer a potential alternative to conventional drug-based treatments and could help address issues related to blood-brain barrier restrictions and adverse drug effects, subject to further validation. Further investigations should address long-term safety, elucidate the mechanistic pathways engaged, and evaluate the feasibility of clinical translation. Collectively, these observations support continued examination of thermal neuromodulation as a potentially valuable direction in AD intervention research.

Materials and Methods

Ethics statement

Animal experiments were conducted according to the regulations approved by the Animal Ethical Committee of National Taiwan University (approval protocol number: NTU-112-EL-00158) Mice were monitored daily for distress, with humane endpoints including reduced social interaction, anorexia, weight loss of 15%, hunching, or inability to evade handling. All hydrodynamic injections

and thermal treatments were conducted under anesthesia with 3% isoflurane (Panion & BF Biotech Inc., Taipei, Taiwan), with utmost care taken to minimize any potential discomfort or distress experienced by the animals. For sacrifice, mice were humanely euthanized via carbon dioxide (CO_2) gas asphyxiation followed by cervical dislocation and considered non-survivors.

Animals

C57BL/6 male mice (6–8 weeks old, 22–26 g) were obtained from National Laboratory Animal Center. Mice were housed in temperature- and humidity-controlled conditions (12/12 light/dark cycle, with the lights on from 7 p.m.–7 a.m. and had free access to a standard diet and drinking water. Animal experiments were conducted according to the ethical policies and procedures approved by the Animal Ethical Committee of National Taiwan University. All mice were randomly assigned into the control, Aβ, FUS-TCS, and FUS-HTS groups. Before applying FUS-TCS or FUS-HTS, the fur on the mice's heads was shaved, and ultrasound transmission gel (TING YU MEDICAL ENTERPRISE CO., LTD., Taichung, Taiwan) was carefully smeared on the interface between the transducer and the mice.

Aβ administration

$A\beta_{25\text{-}35}$ was aggregated into fibrils by incubating it in a 0.9% sterile saline solution at a concentration of 1 mg/mL at 37°C for 7 days. On day 0, 10 μL of the Aβ solution was i.c.v.-injected into the mice's brains in the Aβ, FUS-TCS, and FUS-HTS groups. Meanwhile, 10 μL of sterile saline solution was i.c.v.-injected into the brains of mice in the control group.

Phantom Preparation

A bilayer phantom was fabricated using an acrylamide-based hydrogel to preliminarily evaluate the heating capability of FUS. Briefly, a precursor solution was prepared by mixing 33% (v/v) of a 30% acrylamide stock solution (CAS No. 79-06-1; BioShop Canada Inc., Burlington,

Ontario, Canada) with 61.8% (v/v) deionized water under continuous stirring. Subsequently, 4.5% (v/v) anhydrous glycerol (CAS No. 56-81-5; BioShop, Canada) was added and thoroughly homogenized. Polymerization was initiated by introducing 0.5% (v/v) of 10% ammonium persulfate (CAS No. 7727-54-0; BIO BASIC, Inc., Canada) and 0.2% (v/v) N,N,N',N'-tetramethylethylenediamine (TEMED, CAS No. 110-18-9; Sigma-Aldrich, Merck KGaA). To construct the lateral bilayer configuration, the precursor was evenly divided into two aliquots. One aliquot was supplemented with thermochromic powder (Shenzhen Huancai Color-Changing Technology Co., Ltd.) at a final concentration of 1% (w/v) to produce a white, thermoresponsive region that changes color at 40 °C. A divider was temporary placed in the mold to spatially separate the two compartments. Each formulation was simultaneously cast into its respective section. After partial gelation, the divider was carefully removed to allow interfacial fusion. The phantom was then allowed to polymerize completely under ambient conditions, resulting in a bilayer structure composed of adjacent transparent and thermochromic domains.

FUS-HTS and FUS-TCS applications

Ultrasound sonication was generated by a 1.2 MHz, single-element focused piezoelectric transducer with a diameter of 20 mm and a radius of curvature of 20 mm. A power meter/sensor module (Bird 4421, Bird Electronic Corp., Cleveland, OH) was used to measure the input electrical power. The signal was supplied by a function generator (SG382; Stanford Research Systems, Sunnyvale, CA, USA) and amplified by a power amplifier (25A250, Amplifier Research, Souderton, PA, USA). To measure the actual temperature response of the focal point, a K-type thermocouple was inserted into the brain tissue of the anesthetized mouse during the FUS-TCS and FUS-HTS treatments. For the FUS-TCS application, the right hemisphere of the mice’s brain underwent a 10-cycle repeated procedure treatment, in which each cycle involved activating the FUS for 3 min, followed by a 1 min rest period. In contrast, for the FUS-HTS group, the right hemisphere of the mice’s brain was subjected to FUS treatment for 30 minutes without any rest period intervals. The

FUS-induced temperature elevation in the phantom resulted in visible colorimetric changes were depicted in Figure 1, and the monitored temperatures of mice's brains during FUS-TCS and FUS-HTS applications were shown in Figure 2A.

Experimental schedule design

Mice were randomly assigned to different treatment conditions, including control, FUS-TCS, FUS-HTS, Aβ, Aβ+FUS-TCS, and Aβ+FUS-HTS groups. On day 0, 10 μL of Aβ solution was i.c.v.-injected into the brains of mice in the Aβ, Aβ+FUS-TCS, and Aβ+FUS-HTS groups. In parallel, mice in the control, FUS-TCS, and FUS-HTS groups received an equal volume (10 μL) of PBS via i.c.v. injection as a control treatment. On days 4, 8, and 12, thermal applications were applied to the mice in the FUS-TCS, FUS-HTS, Aβ+FUS-TCS, and Aβ+FUS-HTS groups, as shown in 2A. Following, the locomotor activity, memory, and recognition were assessed via Y-maze and novel object recognition (NOR) tests. These assessments capitalize on mice's innate curiosity to investigate unfamiliar environments or novel objects [38-41]. Y-maze tests were assessed on day 13. NOR tests, including short-term (1 h) and long-term (24 h) assessments, were conducted on days 14 and 15, respectively.

Y-maze test

The Y-maze test was employed to evaluate the spatial working memory of mice. The maze consists of three identical arms (40 cm × 13 cm × 6.5 cm) interconnected at a central junction, with each arm positioned at a 120° angle relative to the others. The mouse under assessment, which was not previously acquainted with the maze, was positioned at the end of the starting arm and allowed unrestricted movement through all three arms for a duration of 8 minutes to evaluate spontaneous alternation. This behavior test is based on mice's intrinsic curiosity to explore all three arms consecutively in a stimulus-free maze, making it an effective measure of spatial working memory [38,39]. After each assessment, olfactory cues in the maze were eliminated using 70% ethanol. The

behavioral performance was recorded, noting the sequence of entries into the three arms designated as "A", "B", and "C". An entry was defined as the hind paws of mice completely entering the arm. A A correct alternation occurs when mice consecutively enter all three arms in overlapping sets, such as A-B-C, A-C-B, B-A-C, B-C-A, C-A-B, and C-B-A. (for example, a pattern of A-C-B-A-C consists of three correct alternations) [38,39]. The spontaneous index was calculated as (number of correct alternations) / (total number of arm entries – 2) × 100. The total number of arm entries reflects the locomotor activity of the mice.

NOR test

The NOR test was used to assess the recognition memory of the animals. The NOR test consists of a habituation phase, a familiarization phase and a test phase. All mice in the habituation phase were placed in a 40 cm × 40 cm × 30.5 cm empty box for 8 min. In the familiarization phase, the assessed mouse was placed in the box for 8 min with 2 identical objects "X" placed close to two diagonal corners of the box. The short-term memory evaluation was carried out 1 h after familiarization phase, the mouse returned to the testing box for the test phase, in which one of the original objects was replaced with a novel object "Y" of a different shape. The mouse's behavioral performance was recorded with an overhead video camera for 8 min. The long-term memory evaluation was performed 24 h later in the same way, but object "Y" was changed to another novel object "Z". After each assessment in all phases, all olfactory cues were removed by 70% ethanol. Exploration was defined as sniffing or manipulating the object with the nose and/or forepaws. The discrimination index was calculated as (Tn-To) / (Tn+To), where Tn and To stand for the exploration time of the novel and original objects, respectively.

Brain tissue collection and Western blot sample preparation

Mice were euthanized by CO_2 gas after the NOR tests on day 15. After confirming the death, their brains were taken out quickly and rinsed with phosphate buffered saline (HyClone; GE

Healthcare Life Sciences, Chicago, IL, USA) supplemented with 1% fresh protease inhibitor cocktail (EMD Millipore, Billerica, MA, USA). The entire hippocampi were swiftly dissected on an ice-cold plate, and kept in ice-cold RIPA lysis buffer (MilliporeSigma, Burlington, MA, USA) supplemented with 1% fresh protease inhibitor cocktail. Subsequently, the hippocampal tissues were homogenized via ultrasound processing (5 sec rectangular pulse with 5 sec interval for 3 times, amplitude 50%, by a Q125 sonicator; Qsonica, Newton, CT, USA) and then centrifuged at 23000×g for 30 min at 4℃. After centrifugation, the supernatants were harvested, and the protein concentration was determined using the Bradford protein assay (BioShop Canada Inc.). Protein samples were stored at -80℃ for subsequent western blotting assessments.

Western blot analysis

Homogenized hippocampi proteins (20 μg) were resolved by sodium dodecyl sulfate polyacrylamide gel electrophoresis and transferred onto polyvinylidene difluoride (PVDF) membranes (MilliporeSigma). Blotted membranes were blocked with 5% bovine serum albumin (BSA) in Tris-buffered saline supplemented with 0.1% Tween-20 (TBST) (BioShop Canada Inc.) for 1 h at room temperature. Subsequently, the membranes were incubated overnight with diluted primary antibodies in blocking buffer at 4 ℃, followed by three rinses with TBST. Primary antibodies employed in this study were anti-Aβ (cat. no. sc-28365; Santa Cruz Biotechnology, Inc., Dallas, TX, USA), anti-IDE (cat. no. ab32216; Abcam, Cambridge, UK), HSP70 (cat. no. 4872; Cell Signaling Technology, Inc.), anti-NEP (cat. no. GTX111680; Gentex, Irvine, CA, USA), anti-SIRT1 (cat. no. 9475; Cell Signaling Technology, Inc.), anti-SOD2 (cat. no. 13141; Cell Signaling Technology, Inc.), and anti-β-actin (cat. no. GTX110564; Gentex). After washing with TBST, the membranes were incubated with horseradish peroxidase-conjugated goat anti-mouse (for probing anti-Aβ primary antibody) (cat. no. ab205719; Abcam) or goat anti-rabbit (for probing the other primary antibodies) secondary antibodies (cat. no. AB_2313567; Jackson ImmunoResearch Laboratories, Inc., West Grove, PA, USA) for 1 h at room temperature. β-actin was used as the

loading control for protein normalization. All the antibodies were diluted to their optimal concentrations as per the manufacturer's recommendations. The protein bands were visualized using an enhanced chemiluminescence substrate (Advansta, San Jose, CA, USA) and captured with an imaging system Amersham Imager 600 (AI600; GE Healthcare Life Sciences). The images were analyzed with Image Lab software (version 6.0.1; Bio-Rad Laboratories, Inc.).

Statistical analysis

All statistical results were shown as mean ±standard error of the mean (SEM) and analyzed using one-way analysis of variance (ANOVA) with Tukey's post hoc test in OriginPro 2022 software (version 2022; OriginLab Corporation, Northampton, MA, USA). P-value < 0.05 indicated a statistically significant difference.

Conclusions

This study reveals that FUS-TCS, which administers mild, localized, and intermittent hyperthermia to the brain, significantly mitigates Aβ-induced cognitive impairments in mice. The treatment induces upregulation of HSP70 and enhances the activity of Aβ-degrading enzymes, including IDE and NEP. Additionally, it elevates the expression of oxidative stress regulators such as SIRT1 and SOD2, indicating a multifaceted neuroprotective mechanism. These results support FUS-TCS as a safe and promising non-pharmacological approach for AD treatment. Future research is warranted to assess the long-term safety, durability of cognitive improvements, and the underlying biological mechanisms across various AD models to determine its translational applicability.

Acknowledgements

We thank the Animal Resource Center and the Consortium of Integrative Biomedical Science Key Technology at National Taiwan University for their technical support.

Funding

The present study was supported by research grants from the Ministry of Science and Technology (grant nos. MOST 110-2112-M-002-004 and MOST 109-2112-M-002-004 to CYC) and the National Science and Technology Council (grant no. NSTC 112-2112-M-002-033 to CYC) of the Republic of China. The funders had no role in the study design, data collection and analysis, decision to publish or preparation of the manuscript.

Data Availability Statement

The data presented in this study are available upon request from the corresponding author.

Author Contributions

Conceptualization, C.-Y.C.; methodology, G.-B.L., H.-H.L. and C.-Y.C.; validation, G.-B.L., H.-H.L., Y.-Y.K., Y.-M.C., F.-T.H., Y.-W.W., Y.K., C.C. and C.-Y.C.; formal analysis, G.-B.L., H.-H.L., Y.-Y.K., Y.-M.C. and C.-Y.C.; investigation, G.-B.L., H.-H.L. and C.-Y.C.; resources, C.-Y.C.; data curation, G.-B.L., H.-H.L., Y.-Y.K., Y.-M.C., F.-T.H., Y.-W.W., Y.K., C.C. and C.-Y.C.; writing—original draft preparation, G.-B.L., and C.-Y.C.; writing—review and editing, G.-B.L. and C.-Y.C.; supervision, C.-Y.C.; funding acquisition, C.-Y.C. All authors have read and agreed to the published version of the manuscript.

Institutional Review Board Statement

All experimental procedures adhered to the established guidelines of the Animal Ethical Committee of National Taiwan University (approval protocol number: NTU-112-EL-00158 (11 November 2024)).

Informed Consent Statement

Not applicable.

Conflicts of Interests

The authors declare that they have no competing interests.

Abbreviations

AD	Alzheimer's disease
Aβ	β-amyloid
BBB	blood-brain barrier
HT	hyperthermia
FUS	focused ultrasound
HIFU	high-intensity focused ultrasound
TC-HT	thermal cycling-hyperthermia
FUS-TCS	focused ultrasound thermal-cycling stimulation
FUS-HTS	focused ultrasound hyperthermia stimulation
i.c.v.	intracerebroventricular
NOR	novel object recognition
HSP70	heat shock protein 70
IDE	insulin-degrading enzyme
NEP	neprilysin
SIRT1	sirtuin 1
SOD2	superoxide dismutase 2
ROS	reactive oxygen species
ANOVA	analysis of variance

References

1. Simon, H.B. Hyperthermia. *N. Engl. J. Med*. **1993**, 329, 483–487. doi: 10.1056/NEJM199308123290708.
2. Hildebrandt, B.; Wust, P.; Ahlers, O.; Dieing, A.; Sreenivasa, G.; Kerner, T.; Felix, R.; Riess, H. The cellular and molecular basis of hyperthermia. *Crit. Rev. Oncol. Hematol*. **2002**, 43, 33–56. doi: 10.1016/s1040-8428(01)00179-2.
3. Moradialvand, M.; Farashi, S.; Deka Dey, A.; Kumar, A.; Sharifi, I.; Hassanpour, M.; Chehelgerdi, M.; Prakash, C.; Kang, H.; Sharifi, E.; et al. Cell fate regulation by hyperthermia: Cancer, stem cells, and immune system. *Alexandria Eng. J.* 2025, 129, 240–254. doi: 10.1016/j.aej.2025.06.022.
4. Klemm, P.; Schulz, N.; Boettger, P.; Lange, U. Heat therapy in rheumatic and musculoskeletal diseases - an overview of clinical and molecular effects. *Int. J. Hyperthermia.* **2024**, 41, 2322667. doi: 10.1080/02656736.2024.2322667.
5. Liebl, C.M.; Kutschan, S.; Dörfler, J.; Käsmann, L.; Hübner, J. Systematic review about complementary medical hyperthermia in oncology. *Clin. Exp. Med.* **2022**, 22, 519–565. doi: 10.1007/s10238-022-00846-9.

6. Smadja, D.M.; Abreu, M.M. Hyperthermia and targeting heat shock proteins: Innovative approaches for neurodegenerative disorders and Long COVID. *Front. Neurosci.* **2025**, 19, 1475376. doi: 10.3389/fnins.2025.1475376.
7. Hunt, A.P.; Minett, G.M.; Gibson, O.R.; Kerr, G.K.; Stewart, I.B. Could heat therapy be an effective treatment for Alzheimer's and Parkinson's diseases? A narrative review. *Front. Physiol.* **2020**, 10, 1556. doi: 10.3389/fphys.2019.01556.
8. Sun, X.; Chen, W.D.; Wang, Y.D. β-Amyloid: The key peptide in the pathogenesis of Alzheimer's disease. *Front. Pharmacol.* **2015**, 6, 221. doi: 10.3389/fphar.2015.00221.
9. Leuner, K.; Schütt, T.; Kurz, C.; Eckert, S.H.; Schiller, C.; Occhipinti, A.; Mai, S.; Jendrach, M.; Eckert, G.P.; Kruse, S.E.; et al. Mitochondrion-derived reactive oxygen species lead to enhanced amyloid beta formation. *Antioxid. Redox Signal.* **2012**, 16, 1421–1433. doi: 10.1089/ars.2011.4173.
10. Miranda, S.; Opazo, C.; Larrondo, L.F.; Muñoz, F.J.; Ruiz, F.; Leighton, F.; Inestrosa, N.C. The role of oxidative stress in the toxicity induced by amyloid beta-peptide in Alzheimer's disease. *Prog. Neurobiol.* **2000**, 62, 633–648. doi: 10.1016/s0301-0082(00)00015-0.
11. Palop, J.J.; Mucke, L. Amyloid-beta-induced neuronal dysfunction in Alzheimer's disease: From synapses toward neural networks. *Nat. Neurosci.* **2010**, 13, 812–818. doi: 10.1038/nn.2583.
12. Yoon, S.S.; Jo, S.A. Mechanisms of amyloid-β peptide clearance: Potential therapeutic targets for Alzheimer's disease. *Biomol. Ther.* **2012**, 20, 245–255. doi: 10.4062/biomolther.2012.20.3.245.
13. Dhapola, R.; Beura, S.K.; Sharma, P.; Singh, S.K.; HariKrishnaReddy, D. Oxidative stress in Alzheimer's disease: Current knowledge of signaling pathways and therapeutics. *Mol. Biol. Rep.* **2024**, 51, 48. doi: 10.1007/s11033-023-09021-z.
14. Zhang, B.; Li, Y.; Li, H.; Shen, X.; Zhu, Z. Therapeutic advances in targeting the amyloid-β pathway for Alzheimer's disease. *Brain Sci.* **2025**, 15, 1101. doi: 10.3390/brainsci15101101.
15. Valle-Medina, A.; Calzada-Mendoza, C.C.; Ocharan-Hernández, M.E.; Jiménez-Zamarripa, C.A.; Juárez-Cedillo, T. Heat shock protein 70 in Alzheimer's disease and other dementias: A possible alternative therapeutic. *J. Alzheimers Dis. Rep.* **2025**, 9, 25424823241307021. doi: 10.1177/25424823241307021.
16. Leak, R.K. Heat shock proteins in neurodegenerative disorders and aging. *J. Cell Commun. Signal.* **2014**, 8, 293–310. doi: 10.1007/s12079-014-0243-9.
17. Miners, J.S.; Barua, N.; Kehoe, P.G.; Gill, S.; Love, S. Aβ-degrading enzymes: Potential for treatment of Alzheimer disease. *J. Neuropathol. Exp. Neurol.* **2011**, 70, 944–959. doi: 10.1097/NEN.0b013e3182345e46.
18. Rizzi, L.; Roriz-Cruz, M. Sirtuin 1 and Alzheimer's disease: An up-to-date review. *Neuropeptides.* **2018**, 71, 54–60. doi: 10.1016/j.npep.2018.07.001.
19. Houldsworth, A. Role of oxidative stress in neurodegenerative disorders: A review of reactive oxygen species and prevention by antioxidants. *Brain Commun*. **2024**, 6, fcad356. doi: 10.1093/braincomms/fcad356.
20. Singh, I.S.; Hasday, J.D. Fever, hyperthermia and the heat shock response. *Int. J. Hyperthermia.* **2013**, 29, 423–435. doi: 10.3109/02656736.2013.808766.
21. Kim, J.Y.; Barua, S.; Huang, M.Y.; Park, J.; Yenari, M.A.; Lee, J.E. Heat shock protein 70 (HSP70) induction: Chaperonotherapy for neuroprotection after brain injury. *Cells.* **2020**, 9, 2020. doi: 10.3390/cells9092020.
22. Tundo, G.R.; Sbardella, D.; Ciaccio, C.; Bianculli, A.; Orlandi, A.; Desimio, M.G.; Arcuri, G.; Coletta, M.; Marini, S. Insulin-degrading enzyme (IDE): A novel heat shock-like protein. *J. Biol. Chem.* **2013**, 288, 2281–2289. doi: 10.1074/jbc.M112.393108.
23. Laukkanen, T.; Kunutsor, S.; Kauhanen, J.; Laukkanen, J.A. Sauna bathing is inversely associated with dementia and Alzheimer's disease in middle-aged Finnish men. *Age Ageing.* **2017**, 46, 245–249. doi: 10.1093/ageing/afw212.
24. Labib, S.; Bright, R.K.; Liu, J. Focused ultrasound in cancer immunotherapy: A review of mechanisms and applications. *Ultrasound Med. Biol.* **2025**, 51, 1–14. doi: 10.1016/j.ultrasmedbio.2024.09.008.
25. De Maio, A.; Alfieri, G.; Mattone, M.; Ghanouni, P.; Napoli, A. High-intensity focused ultrasound surgery for tumor ablation: A review of current applications. *Radiol. Imaging Cancer*. **2024**, 6, e230074. doi: 10.1148/rycan.230074.
26. Kennedy, J.E. High-intensity focused ultrasound in the treatment of solid tumours. *Nat. Rev. Cancer.* **2005**, 5, 321–327. doi: 10.1038/nrc1591.

27. Lio, M.L.; Chang, C.C.; Chuang, A.D.; Tsai, L.C.; Chen, C.C. Quantified facial rejuvenation utilizing high intense focus ultrasound with multiple penetrative depths. *Clin. Cosmet. Investig. Dermatol.* **2022**, 15, 489–496. doi: 10.2147/CCID.S350556.
28. Haykal, D.; Sattler, S.; Verner, I.; Madhumita, M.; Cartier, H. A systematic review of high-intensity focused ultrasound in skin tightening and body contouring. *Aesthet. Surg. J.* **2025**, 45, 690–698. doi: 10.1093/asj/sjaf053.
29. Cox, S.S.; Connolly, D.J.; Peng, X.; Badran, B.W. A comprehensive review of low-intensity focused ultrasound parameters and applications in neurologic and psychiatric disorders. *Neuromodulation.* **2025**, 28, 1–15. doi: 10.1016/j.neurom.2024.07.008.
30. Kong, C.; Chang, W.S. Preclinical research on focused ultrasound-mediated blood–brain barrier opening for neurological disorders: A review. *Neurol. Int.* **2023**, 15, 285–300. doi: 10.3390/neurolint15010018.
31. Cheng, B.; Bing, C.; Chu, T.H.; Alzahrani, S.; Pichardo, S.; Pike, G.B. Simultaneous localized brain mild hyperthermia and blood–brain barrier opening via feedback-controlled transcranial MR-guided focused ultrasound and microbubbles. *IEEE Trans. Biomed. Eng.* **2022**, 69, 1880–1888. doi: 10.1109/TBME.2021.3130164.
32. Chan, H.; Chang, H.Y.; Lin, W.L.; Chen, G.S. Large-volume focused-ultrasound mild hyperthermia for improving blood–brain tumor barrier permeability application. *Pharmaceutics.* **2022**, 14, 2012. doi: 10.3390/pharmaceutics14102012.
33. Lee, W.; Moon, M.; Kim, H.G.; Lee, T.H.; Oh, M.S. Heat stress-induced memory impairment is associated with neuroinflammation in mice. *J. Neuroinflammation*. **2015**, 12, 102. doi: 10.1186/s12974-015-0324-6.
34. Kiyatkin, E.A. Brain hyperthermia during physiological and pathological conditions: Causes, mechanisms, and functional implications. *Curr. Neurovasc. Res.* **2004**, 1, 77–90. doi: 10.2174/1567202043480233.
35. Chen, W.T.; Kuo, Y.Y.; Lin, G.B.; Lu, C.H.; Hsu, H.P.; Sun, Y.K.; Chao, C.Y. Thermal cycling protects SH-SY5Y cells against hydrogen peroxide and β-amyloid-induced cell injury through stress response mechanisms involving Akt pathway. *PLoS One.* **2020**, 15, e0240022. doi: 10.1371/journal.pone.0240022.
36. Kuo, Y.Y.; Lin, G.B.; Chen, Y.M.; Liu, H.H.; Hsu, F.T.; Kung, Y.; Chao, C.Y. Thermal cycling-hyperthermia attenuates rotenone-induced cell injury in SH-SY5Y cells through heat-activated mechanisms. *Int. J. Mol. Sci.* **2025**, 26, 6671. doi: 10.3390/ijms26146671.
37. Kuo, Y.Y.; Chen, W.T.; Lin, G.B.; Chen, Y.M.; Liu, H.H.; Chao, C.Y. Thermal cycling-hyperthermia ameliorates Aβ25–35-induced cognitive impairment in C57BL/6 mice. *Neurosci. Lett.* **2023**, 810, 137337. doi: 10.1016/j.neulet.2023.137337.
38. Prieur, E.A.K.; Jadavji, N.M. Assessing spatial working memory using the spontaneous alternation Y-maze test in aged male mice. *Bio Protoc.* **2019**, 9, e3162. doi: 10.21769/BioProtoc.3162.
39. Kraeuter, A.K.; Guest, P.C.; Sarnyai, Z. The Y-maze for assessment of spatial working and reference memory in mice. *Methods Mol. Biol.* **2019**, 1916, 105–111. doi: 10.1007/978-1-4939-8994-2_10.
40. Lueptow, L.M. Novel object recognition test for the investigation of learning and memory in mice. *J. Vis. Exp.* **2017**, 126, 55718. doi: 10.3791/55718.
41. Navarro, D.; Gasparyan, A.; Martí Martínez, S.; Díaz Marín, C.; Navarrete, F.; García Gutiérrez, M.S.; Manzanares, J. Methods to identify cognitive alterations from animals to humans: A translational approach. *Int. J. Mol. Sci.* **2023**, 24, 7653. doi: 10.3390/ijms24087653.
42. Tian, Y.; Jing, G.; Zhang, M. Insulin-degrading enzyme: Roles and pathways in ameliorating cognitive impairment associated with Alzheimer's disease and diabetes. *Ageing Res. Rev.* **2023**, 90, 101999. doi: 10.1016/j.arr.2023.101999.
43. Cerasuolo, M.; Auriemma, M.C.; Di Meo, I.; Lenti, C.; Papa, M.; Paolisso, G.; Rizzo, M.R. Understanding the insulin-degrading enzyme: A new look at Alzheimer's disease and Aβ plaque management. *Int. J. Mol. Sci.* **2025**, 26, 6693. doi: 10.3390/ijms26146693.
44. Saxena, S.K.; Ansari, S.; Maurya, V.K.; Kumar, S.; Sharma, D.; Malhotra, H.S.; Tiwari, S.; Srivastava, C.; Paweska, J.T.; Abdel-Moneim, A.S.; et al. Neprilysin-mediated amyloid beta clearance and its therapeutic implications in neurodegenerative disorders. *ACS Pharmacol. Transl. Sci.* **2024**, 7, 3645–3657. doi: 10.1021/acsptsci.4c00400.
45. Grimm, M.O.; Mett, J.; Stahlmann, C.P.; Haupenthal, V.J.; Zimmer, V.C.; Hartmann, T. Neprilysin and Aβ clearance: Impact of the APP intracellular domain in NEP regulation and implications in Alzheimer's disease. Front. *Aging Neurosci*. **2013**, 5, 98. doi: 10.3389/fnagi.2013.00098.

46. Morito, T.; Hashimoto, S.; Takamura, R.; Watamura, N.; Kakiya, N.; Fujioka, R.; Mihara, N.; Sekiguchi, M.; Watanabe-Iwata, K.; Kamano, N.; et al. The role of neprilysin and insulin-degrading enzyme in the etiology of sporadic Alzheimer's disease. *J. Neurosci.* **2025**, 45, e2152242025. doi: 10.1523/JNEUROSCI.2152-24.2025.
47. Park, M.H.; Lee, J.K.; Choi, S.; Ahn, J.; Jin, H.K.; Park, J.S.; Bae, J.S. Recombinant soluble neprilysin reduces amyloid-beta accumulation and improves memory impairment in Alzheimer's disease mice. *Brain Res.* **2013**, 1529, 113–124. doi: 10.1016/j.brainres.2013.05.045.
48. Nalivaeva, N.N.; Belyaev, N.D.; Zhuravin, I.A.; Turner, A.J. The Alzheimer's amyloid-degrading peptidase, neprilysin: Can we control it? *Int. J. Alzheimers Dis.* **2012**, 2012, 383796. doi: 10.1155/2012/383796.
49. Bhatt, S.; Puli, L.; Patil, C.R. Role of reactive oxygen species in the progression of Alzheimer's disease. *Drug Discov. Today*. **2021**, 26, 794–803. doi: 10.1016/j.drudis.2020.12.004.
50. Huang, W.J.; Zhang, X.; Chen, W.W. Role of oxidative stress in Alzheimer's disease. *Biomed. Rep.* **2016**, 4(5), 519–522. doi: 10.3892/br.2016.630.
51. Zhao, Y.; Zhao, B. Oxidative stress and the pathogenesis of Alzheimer's disease. *Oxid. Med. Cell. Longev.* **2013**, 2013, 316523. doi: 10.1155/2013/316523.
52. Singh, C.K.; Chhabra, G.; Ndiaye, M.A.; Garcia-Peterson, L.M.; Mack, N.J.; Ahmad, N. The role of sirtuins in antioxidant and redox signaling. *Antioxid. Redox Signal.* **2018**, 28, 643–661. doi: 10.1089/ars.2017.7290.
53. Hwang, J.W.; Yao, H.; Caito, S.; Sundar, I.K.; Rahman, I. Redox regulation of SIRT1 in inflammation and cellular senescence. *Free Radic. Biol. Med.* **2013**, 61, 95–110. doi: 10.1016/j.freeradbiomed.2013.03.015.
54. Lutz, M.I.; Milenkovic, I.; Regelsberger, G.; Kovacs, G.G. Distinct patterns of sirtuin expression during progression of Alzheimer's disease. *Neuromolecular Med.* **2014**, 16, 405–414. doi: 10.1007/s12017-014-8288-8.
55. Julien, C.; Tremblay, C.; Emond, V.; Lebbadi, M.; Salem, N. Jr; Bennett, D.A.; Calon, F. Sirtuin 1 reduction parallels the accumulation of tau in Alzheimer disease. *J. Neuropathol. Exp. Neurol.* **2009**, 68, 48–58. doi: 10.1097/NEN.0b013e3181922348.
56. Corpas, R.; Revilla, S.; Ursulet, S.; Castro-Freire, M.; Kaliman, P.; Petegnief, V.; Giménez-Llort, L.; Sarkis, C.; Pallàs, M.; Sanfeliu, C. SIRT1 overexpression in mouse hippocampus induces cognitive enhancement through proteostatic and neurotrophic mechanisms. *Mol. Neurobiol.* **2017**, 54, 5604–5619. doi: 10.1007/s12035-016-0087-9.
57. Koo, J.H.; Kang, E.B.; Oh, Y.S.; Yang, D.S.; Cho, J.Y. Treadmill exercise decreases amyloid-β burden possibly via activation of SIRT-1 signaling in a mouse model of Alzheimer's disease. *Exp. Neurol.* **2017**, 288, 142–152. doi: 10.1016/j.expneurol.2016.11.014.
58. Qin, W.; Yang, T.; Ho, L.; Zhao, Z.; Wang, J.; Chen, L.; Zhao, W.; Thiyagarajan, M.; MacGrogan, D.; Rodgers, J.T.; et al. Neuronal SIRT1 activation as a novel mechanism underlying the prevention of Alzheimer disease amyloid neuropathology by calorie restriction. *J. Biol. Chem.* **2006**, 281, 21745–21754. doi: 10.1074/jbc.M602909200.
59. Zhang, W.; Zhang, Y.; Guo, X.; Zeng, Z.; Wu, J.; Liu, Y.; He, J.; Wang, R.; Huang, Q.; Chen, Z. Sirt1 protects endothelial cells against LPS-induced barrier dysfunction. *Oxid. Med. Cell Longev.* **2017**, 2017, 4082102. doi: 10.1155/2017/4082102.
60. Cheng, Y.; Takeuchi, H.; Sonobe, Y.; Jin, S.; Wang, Y.; Horiuchi, H.; Parajuli, B.; Kawanokuchi, J.; Mizuno, T.; Suzumura, A. Sirtuin 1 attenuates oxidative stress via upregulation of superoxide dismutase 2 and catalase in astrocytes. *J. Neuroimmunol.* **2014**, 269, 38–43. doi: 10.1016/j.jneuroim.2014.02.001.
61. Khan, R.S.; Fonseca-Kelly, Z.; Callinan, C.; Zuo, L.; Sachdeva, M.M.; Shindler, K.S. SIRT1 activating compounds reduce oxidative stress and prevent cell death in neuronal cells. *Front. Cell Neurosci.* **2012**, 6, 63. doi: 10.3389/fncel.2012.00063.
62. Massaad, C.A.; Washington, T.M.; Pautler, R.G.; Klann, E. Overexpression of SOD-2 reduces hippocampal superoxide and prevents memory deficits in a mouse model of Alzheimer's disease. *Proc. Natl. Acad. Sci. U.S.A.* **2009**, 106, 13576–13581. doi: 10.1073/pnas.0902714106.
63. Zhang, Y.; Chen, H.; Li, R.; Sterling, K.; Song, W. Amyloid β-based therapy for Alzheimer's disease: challenges, successes and future. *Signal Transduct. Target Ther.* **2023**, 8, 248. doi: 10.1038/s41392-023-01484-7.
64. Chen, G.F.; Xu, T.H.; Yan, Y.; Zhou, Y.R.; Jiang, Y.; Melcher, K.; Xu, H.E. Amyloid beta: structure, biology and structure-based therapeutic development. *Acta Pharmacol. Sin.* **2017**, 38, 1205–1235. doi: 10.1038/aps.2017.28.
65. Wu, D.; Chen, Q.; Chen, X.; Han, F.; Chen, Z.; Wang, Y. The blood-brain barrier: structure, regulation, and drug delivery. *Signal Transduct. Target Ther.* **2023**, 8, 217. doi: 10.1038/s41392-023-01481-w.

66. Pardridge, W.M. Alzheimer's disease drug development and the problem of the blood-brain barrier. *Alzheimers Dement.* **2009**, 5, 427–432. doi: 10.1016/j.jalz.2009.06.003.
67. Hunt, A.P.; Minett, G.M.; Gibson, O.R.; Kerr, G.K.; Stewart, I.B. Could heat therapy be an effective treatment for Alzheimer's and Parkinson's diseases? A narrative review. *Front. Physiol.* **2020**, 10, 1556. doi: 10.3389/fphys.2019.01556.
68. Von Schulze, A.T.; Deng, F.; Morris, J.K.; Geiger, P.C. Heat therapy: possible benefits for cognitive function and the aging brain. *J. Appl. Physiol.* **2020**, 129, 1468–1476. doi: 10.1152/japplphysiol.00168.2020.
69. Rivera, I.; Capone, R.; Cauvi, D.M.; Arispe, N.; De Maio, A. Modulation of Alzheimer's amyloid β peptide oligomerization and toxicity by extracellular Hsp70. *Cell Stress Chaperones.* **2018**, 23, 269–279. doi: 10.1007/s12192-017-0839-0.
70. Lu, R.C.; Tan, M.S.; Wang, H.; Xie, A.M.; Yu, J.T.; Tan, L. Heat shock protein 70 in Alzheimer's disease. *Biomed. Res. Int.* **2014**, 2014, 435203. doi: 10.1155/2014/435203.
71. Yun, Y.J.; Park, B.H.; Hou, J.; Oh, J.P.; Han, J.H.; Kim, S.C. Ginsenoside F1 protects the brain against amyloid beta-induced toxicity by regulating IDE and NEP. *Life (Basel).* **2022**, 12, 58. doi: 10.3390/life12010058.
72. Leissring, M.A.; Farris, W.; Chang, A.Y.; Walsh, D.M.; Wu, X.; Sun, X.; Frosch, M.P.; Selkoe, D.J. Enhanced proteolysis of beta-amyloid in APP transgenic mice prevents plaque formation, secondary pathology, and premature death. *Neuron.* **2003**, 40, 1087–1093. doi: 10.1016/s0896-6273(03)00787-6.
73. Vekrellis, K.; Ye, Z.; Qiu, W.Q.; Walsh, D.; Hartley, D.; Chesneau, V.; Rosner, M.R.; Selkoe, D.J. Neurons regulate extracellular levels of amyloid beta-protein via proteolysis by insulin-degrading enzyme. *J. Neurosci.* **2000**, 20, 1657–1665. doi: 10.1523/JNEUROSCI.20-05-01657.2000.
74. Salminen, A.; Kaarniranta, K.; Kauppinen, A. Crosstalk between oxidative stress and SIRT1: impact on the aging process. *Int. J. Mol. Sci.* **2013**, 14, 3834–3859. doi: 10.3390/ijms14023834.
75. Mishra, P.; Mittal, A.K.; Kalonia, H.; Madan, S.; Ghosh, S.; Sinha, J.K.; Rajput, S.K. SIRT1 promotes neuronal fortification in neurodegenerative diseases through attenuation of pathological hallmarks and enhancement of cellular lifespan. *Curr. Neuropharmacol.* **2021**, 19, 1019–1037. doi: 10.2174/1570159X18666200729111744.
76. Kumar, R.; Chaterjee, P.; Sharma, P.K.; Singh, A.K.; Gupta, A.; Gill, K.; Tripathi, M.; Dey, A.B.; Dey, S. Sirtuin1: a promising serum protein marker for early detection of Alzheimer's disease. *PLoS One*. **2013**, 8, e61560. doi: 10.1371/journal.pone.0061560.
77. Hadar, A.; Milanesi, E.; Walczak, M.; Puzianowska-Kuźnicka, M.; Kuźnicki, J.; Squassina, A.; Niola, P.; Chillotti, C.; Attems, J.; Gozes, I.; et al. SIRT1, miR-132 and miR-212 link human longevity to Alzheimer's disease. *Sci. Rep.* **2018**, 8, 8465. doi: 10.1038/s41598-018-26547-6.
78. Zhu, L.; Lu, F.; Zhang, X.; Liu, S.; Mu, P. SIRT1 is involved in the neuroprotection of pterostilbene against amyloid β 25-35-induced cognitive deficits in mice. *Front. Pharmacol.* **2022**, 13, 877098. doi: 10.3389/fphar.2022.877098.
79. Kaszubowska, L.; Foerster, J.; Kaczor, J.J.; Schetz, D.; Ślebioda, T.J.; Kmieć, Z. Expression of cellular protective proteins SIRT1, HSP70 and SOD2 correlates with age and is significantly higher in NK cells of the oldest seniors. *Immun Ageing.* **2017**, 14, 3. doi: 10.1186/s12979-017-0085-4.
80. Petrofsky, J.; Berk, L.; Bains, G.; Khowailed, I.A.; Lee, H.; Laymon, M. The efficacy of sustained heat treatment on delayed-onset muscle soreness. *Clin. J. Sport Med.* **2017**, 27, 329–337. doi: 10.1097/JSM.0000000000000375.
81. Yi, G.Y.; Kim, M.J.; Kim, H.I.; Park, J.; Baek, S.H. Hyperthermia treatment as a promising anti-cancer strategy: therapeutic targets, perspective mechanisms and synergistic combinations in experimental approaches. *Antioxidants (Basel).* **2022**, 11, 625. doi: 10.3390/antiox11040625.
82. Wang, Y.; Xun, X.; Luan, W.Y.; Zhang, Z.; Xu, Z.X.; Lin, S.X.; Miao, Y.D. Hyperthermia combined with opioid therapy: enhancing cancer pain management and reducing surgical stress in gastrointestinal cancer patients. *World J. Gastrointest. Surg.* **2025**, 17, 101060. doi: 10.4240/wjgs.v17.i3.101060.

Figure 1

A

B

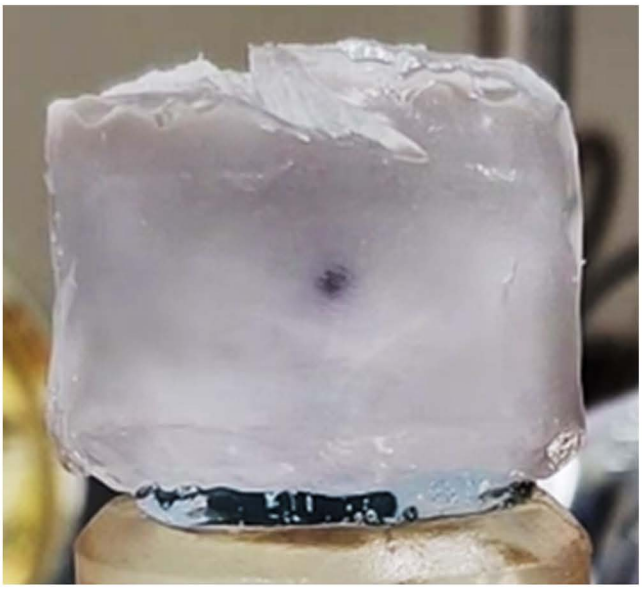

C

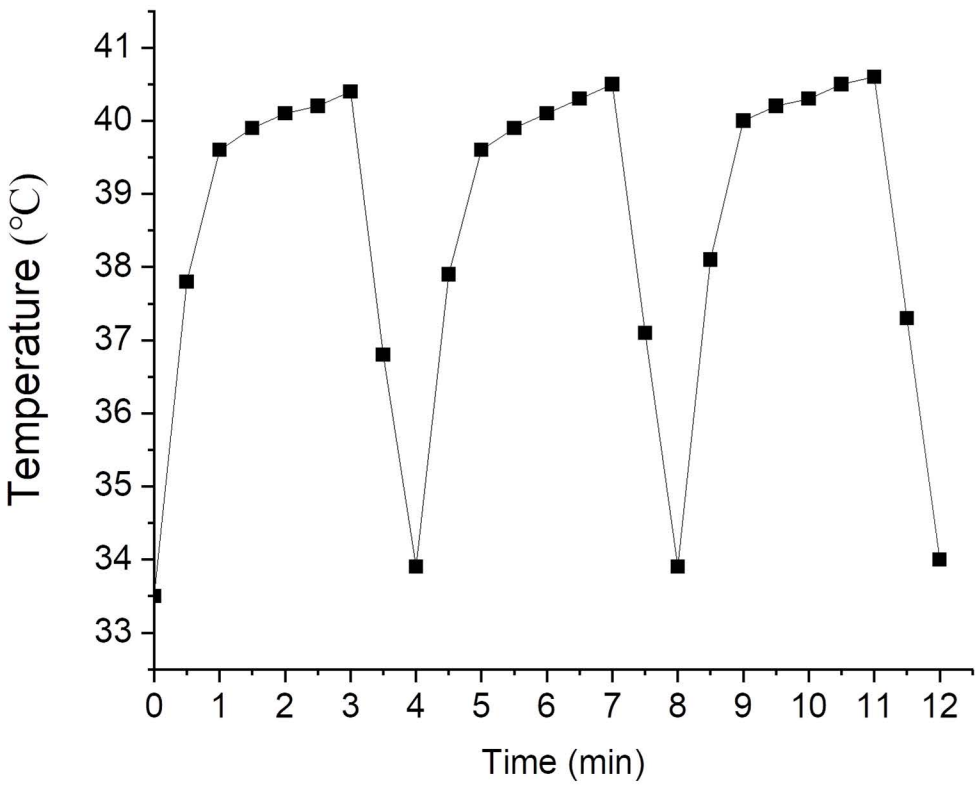
Temperature (°C)
41
40
39
38
37
36
35
34
33
0
1
2
3
4
5
6
7
8
9
10
11
12
Time (min)

Figure 2

A

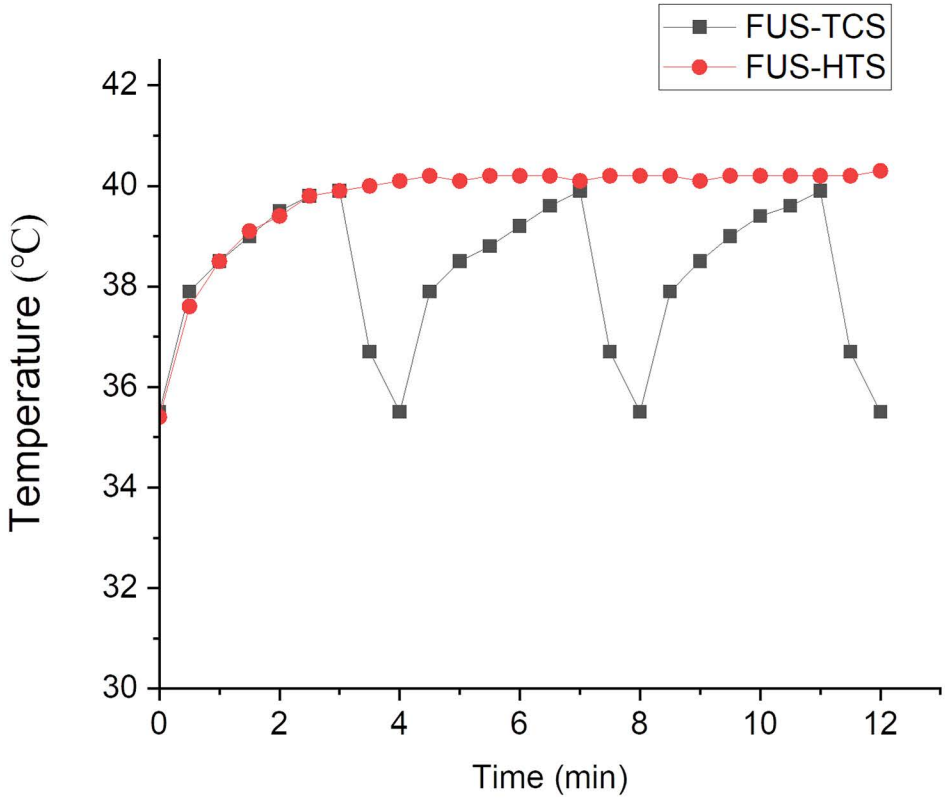
FUS-TCS
FUS-HTS
Temperature (°C)
42
40
38
36
34
32
30
0
2
4
6
8
10
12
Time (min)

B

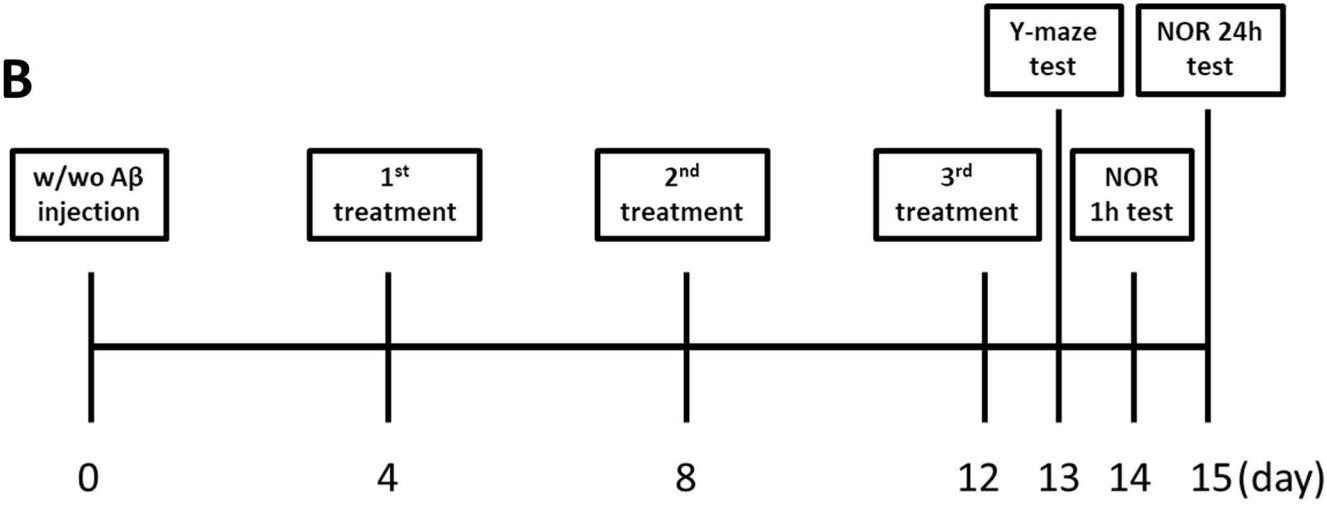
Y-maze test
NOR 24h test
w/wo Aβ injection
1st treatment
2nd treatment
3rd treatment
NOR 1h test
0
4
8
12
13
14
15 (day)

Figure 3

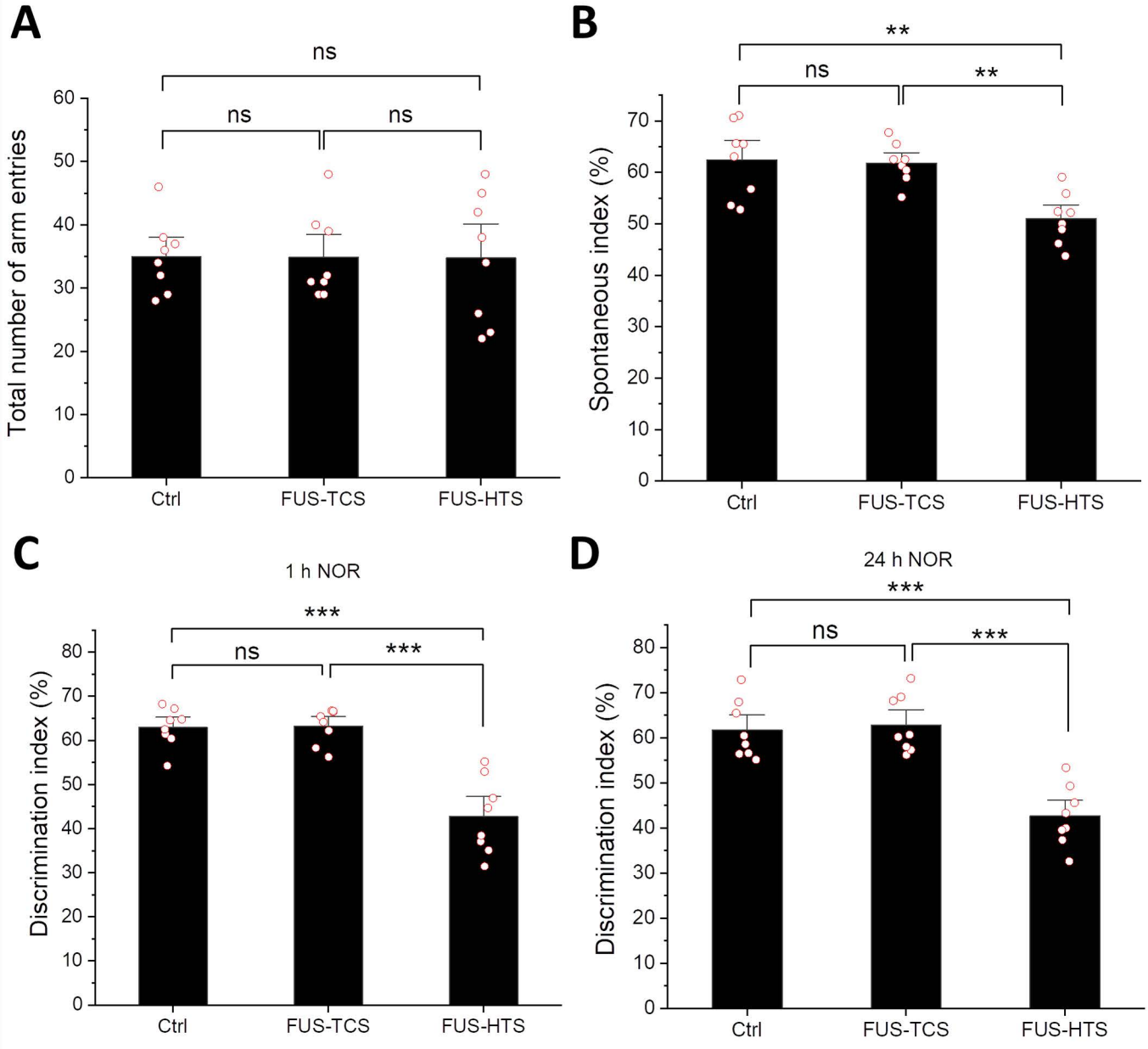
A
ns
ns
ns
Total number of arm entries
0
10
20
30
40
50
60
Ctrl
FUS-TCS
FUS-HTS
B
**
ns
**
Spontaneous index (%)
0
10
20
30
40
50
60
70
Ctrl
FUS-TCS
FUS-HTS
C
1 h NOR
***
ns
***
Discrimination index (%)
0
10
20
30
40
50
60
70
80
Ctrl
FUS-TCS
FUS-HTS
D
24 h NOR
***
ns
***
Discrimination index (%)
0
10
20
30
40
50
60
70
80
Ctrl
FUS-TCS
FUS-HTS

Figure 4

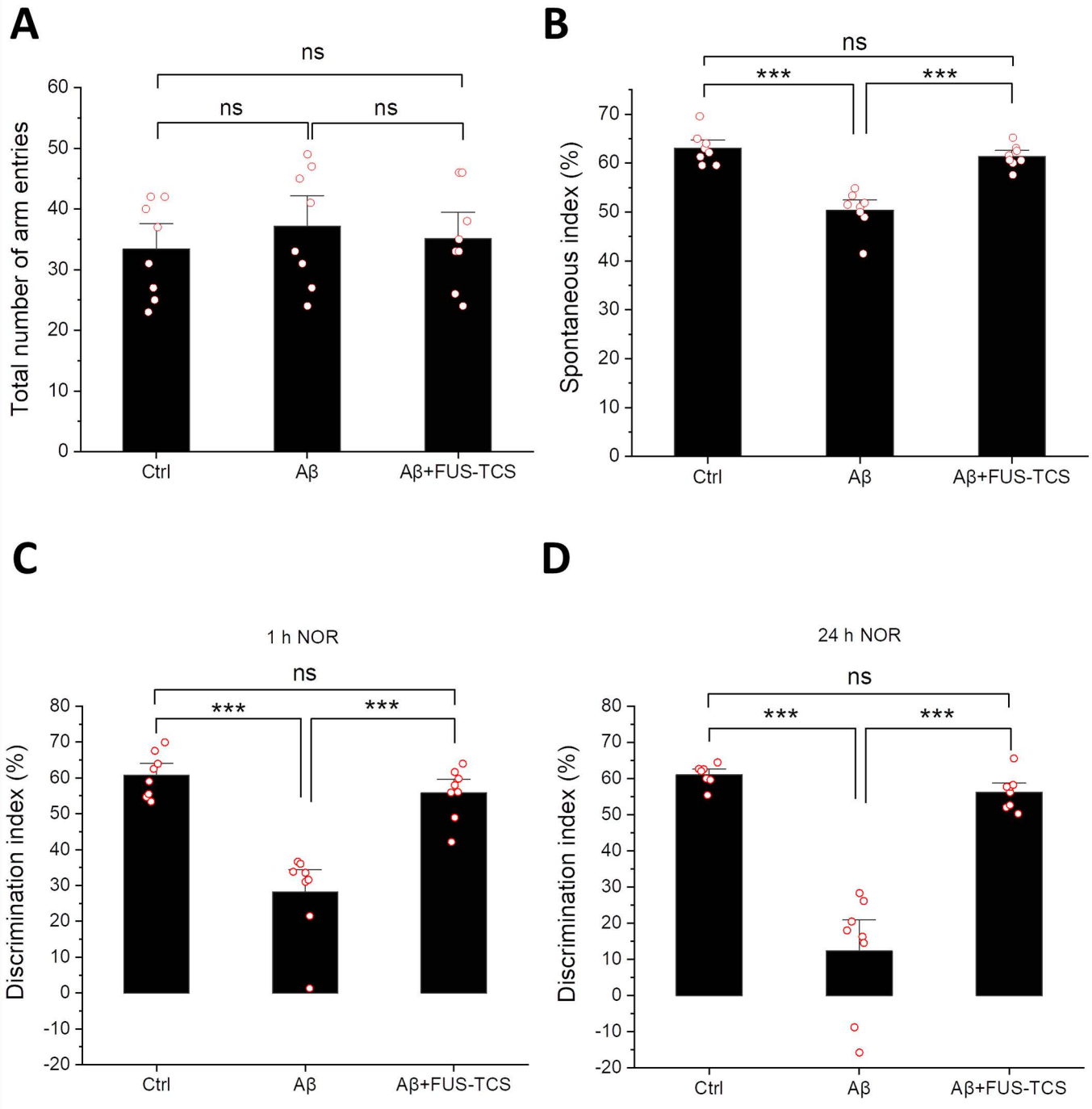
A
ns
ns
ns
Total number of arm entries
0
10
20
30
40
50
60
Ctrl
Aβ
Aβ+FUS-TCS
B
ns
***
***
Spontaneous index (%)
0
10
20
30
40
50
60
70
Ctrl
Aβ
Aβ+FUS-TCS
C
1 h NOR
ns
***
***
Discrimination index (%)
-20
-10
0
10
20
30
40
50
60
70
80
Ctrl
Aβ
Aβ+FUS-TCS
D
24 h NOR
ns
***
***
Discrimination index (%)
-20
-10
0
10
20
30
40
50
60
70
80
Ctrl
Aβ
Aβ+FUS-TCS

Figure 5

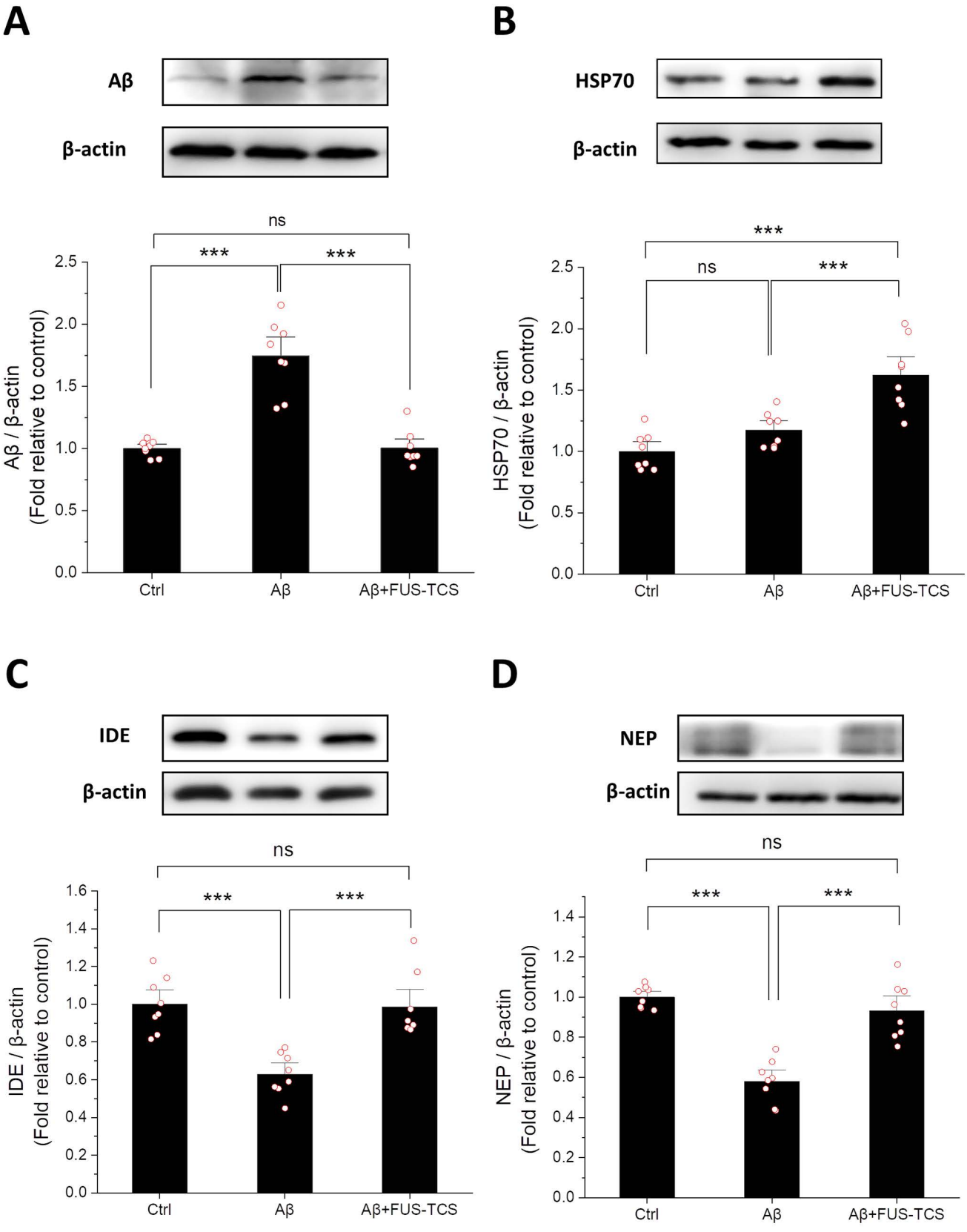
A
Aβ
β-actin
ns
***
***
Aβ / β-actin
(Fold relative to control)
2.5
2.0
1.5
1.0
0.5
0.0
Ctrl
Aβ
Aβ+FUS-TCS
B
HSP70
β-actin
***
ns
***
HSP70 / β-actin
(Fold relative to control)
2.5
2.0
1.5
1.0
0.5
0.0
Ctrl
Aβ
Aβ+FUS-TCS
C
IDE
β-actin
ns
***
***
IDE / β-actin
(Fold relative to control)
1.6
1.4
1.2
1.0
0.8
0.6
0.4
0.2
0.0
Ctrl
Aβ
Aβ+FUS-TCS
D
NEP
β-actin
ns
***
***
NEP / β-actin
(Fold relative to control)
1.4
1.2
1.0
0.8
0.6
0.4
0.2
0.0
Ctrl
Aβ
Aβ+FUS-TCS

Figure 6

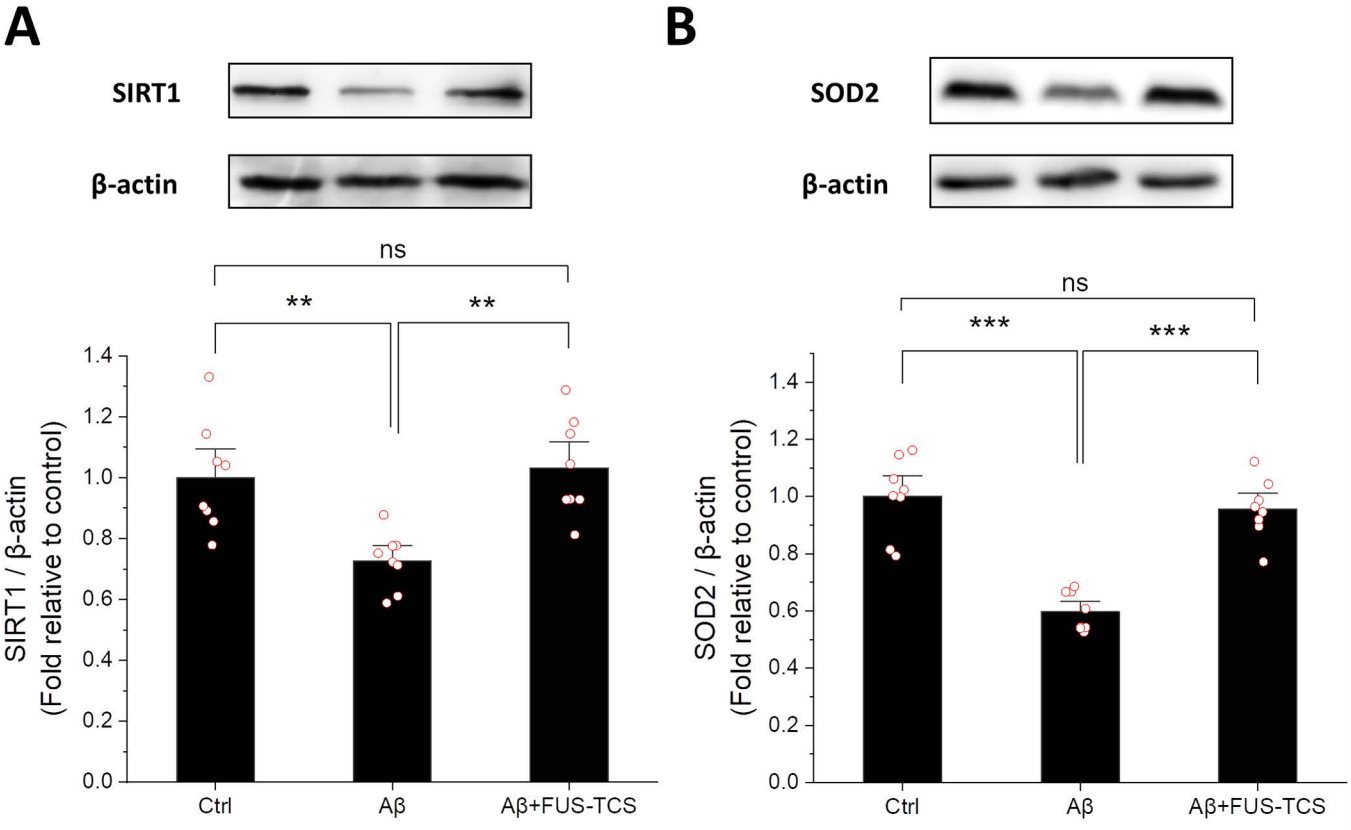
A
SIRT1
β-actin
ns
**
**
SIRT1 / β-actin
(Fold relative to control)
1.4
1.2
1.0
0.8
0.6
0.4
0.2
0.0
Ctrl
Aβ
Aβ+FUS-TCS
B
SOD2
β-actin
ns
***
***
SOD2 / β-actin
(Fold relative to control)
1.4
1.2
1.0
0.8
0.6
0.4
0.2
0.0
Ctrl
Aβ
Aβ+FUS-TCS